JOURNAL OF AIRCRAFT
Vol. 41, No. 3, May–June 2004

High-Fidelity Aerostructural Design Optimization of a Supersonic Business Jet

Joaquim R. R. A. Martins*
University of Toronto Institute for Aerospace Studies, Toronto, Ontario M3H 5T6, Canada
Juan J. Alonso†
Stanford University, Stanford, California 94305
and
James J. Reuther‡
NASA Ames Research Center, Moffett Field, California 95035

This paper focuses on the demonstration of an integrated aerostructural method for the design of aerospace vehicles. Both aerodynamics and structures are represented using high-fidelity models such as the Euler equations for the aerodynamics and a detailed finite element model for the primary structure. The aerodynamic outer-mold line and a structure of fixed topology are parameterized using a large number of design variables. The aerostructural sensitivities of aerodynamic and structural cost functions with respect to both outer-mold line shape and structural variables are computed using an accurate and efficient coupled-adjoint procedure. Kreisselmeier–Steinhauser functions are used to reduce the number of structural constraints in the problem. Results of the aerodynamic shape and structural optimization of a natural laminar-flow supersonic business jet are presented together with an assessment of the accuracy of the sensitivity information obtained using the coupled-adjoint procedure.

Introduction

A CONSIDERABLE amount of research has been conducted on multidisciplinary design optimization (MDO) and its application to aircraft design. The survey papers by Sobieszczanski-Sobieski and Haftka[1] and Alexandrov and Hussaini[2] provide a comprehensive discussion of much of the work in this area. The efforts described therein range from the development of techniques for interdisciplinary coupling to applications in real-world design problems. In most cases sound coupling and optimization methods were shown to be extremely important because some techniques, such as sequential discipline optimization, were unable to converge to the true optimum of a coupled system. Wakayama,[3] for example, showed that in order to obtain realistic wing planform shapes with aircraft design optimization it is necessary to include multiple disciplines in conjunction with a complete set of realistic constraints.

Aerostructural analysis has traditionally been carried out in a cut-and-try basis. Aircraft designers have a preconceived idea of the shape of an "optimal" load distribution and then tailor the jig shape of the structure so that the deflected wing shape under a 1-g load gives the desired load distribution. Although this approach might suffice for conventional transport aircraft, for which there is considerable accumulated experience, in the case of either new planform concepts or new flight regimes the lack of experience combined with the complexities of aerostructural interactions can lead to designs that are far from optimal.

This is certainly the case in the design of supersonic transports, where simple beam theory models of the wing cannot be used to accurately describe the behavior of the wing structure. In some cases these aircraft must even cruise for significant portions of their flight at different Mach numbers. In addition, a variety of studies show that supersonic transports exhibit a range of undesirable aeroelastic phenomena because of the low bending and torsional stiffness that result from wings with low thickness-to-chord ratio. These phenomena can only be suppressed when aerostructural interactions are taken into account at the preliminary design stage.[4]

Unfortunately, the modeling of the participating disciplines in most of the work that has appeared so far has remained at a relatively low level. Although useful at the conceptual design stage, lower-order models cannot accurately represent a variety of nonlinear phenomena such as wave drag, which can play an important role in the search for the optimum design. An exception to low-fidelity modeling is the recent work by Giunta[5] and by Maute et al.,[6] where aerostructural sensitivities are calculated using higher-fidelity models.

The ultimate objective of our work is to develop an MDO framework for high-fidelity analysis and optimization of aircraft configurations. The framework is built upon prior work by the authors on aerostructural high-fidelity sensitivity analysis.[7–10] The objective of this paper is to present the current capability of this framework and to demonstrate it by performing the aerostructural design of a supersonic business-jet configuration.

The following sections begin with the description of the aircraft optimization problem we propose to solve. We then introduce the general formulation of the sensitivity equations followed by the description of the specific case of the adjoint equations for the aerostructural system. A detailed study of the accuracy of the aerostructural sensitivity information is also presented for validation purposes. Finally, we present results of the application of our sensitivity analysis method to the full aerostructural optimization of a supersonic business jet and compare the results with the more traditional approach of sequential discipline optimizations, where we highlight the fact that only truly coupled optimization frameworks yield the true optimum of the system.

Aircraft Optimization Problem

For maximum lift-to-drag ratio it is a well-known result from classical subsonic aerodynamics that a wing must exhibit an elliptic lift distribution in the spanwise direction. For aircraft design, however, it is usually not the lift-to-drag ratio we want to maximize

Presented as Paper 2002-1483 at the AIAA/ASME/ASCE/AHS/ASC 43rd Structures, Structural Dynamics, and Material Conference, Denver, CO, 22–25 April 2002; received 25 June 2002; revision received 30 April 2003; accepted for publication 20 June 2003.

*Assistant Professor. Member AIAA.
†Assistant Professor. Member AIAA.
‡Research Scientist. Associate Fellow AIAA.

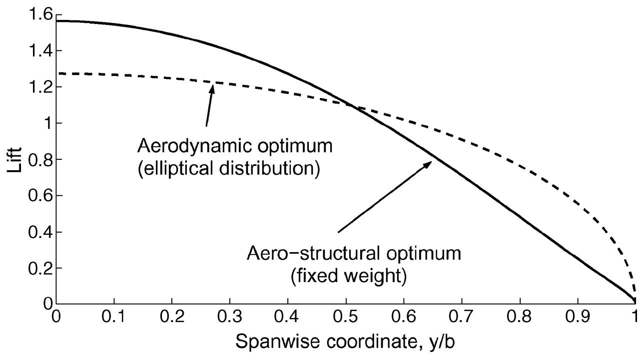

Fig. 1 Elliptic vs aerostructural optimum lift distribution.

Fig. 2 Natural laminar-flow supersonic business-jet configuration.

but an objective function that reflects the overall mission of the particular aircraft. Consider, for example, the Breguet range formula for jet-powered aircraft:

$$\text{Range} = \frac{V}{c}\frac{C_L}{C_D}\ln\frac{W_i}{W_f} \tag{1}$$

where V is the cruise velocity and c is the thrust-specific fuel consumption of the powerplant. C_L/C_D is the ratio of lift to drag, and W_i/W_f is the ratio of initial and final cruise weights of the aircraft.

The Breguet range equation expresses a tradeoff between the drag and the empty weight of the aircraft and constitutes a reasonable objective function to use in aircraft design. If we were to parameterize a design with both aerodynamic and structural design variables and then maximize the range for a fixed initial cruise weight, subject to stress constraints, we would obtain a lift distribution similar to the one shown in Fig. 1.

This optimum lift distribution trades off the drag penalty associated with unloading the tip of the wing, where the loading contributes most to the maximum stress at the root of the wing structure in order to reduce the weight. The end result is an increase in range when compared to the elliptically loaded wing because of a higher weight fraction W_i/W_f. The result shown in Fig. 1 illustrates the need for taking into account the coupling of aerodynamics and structures when performing aircraft design.

The aircraft configuration used in this work is the supersonic business jet shown in Fig. 2. This configuration is being developed by the ASSET Research Corporation and is designed to achieve a large percentage of laminar flow on the low-sweep wing, resulting in decreased friction drag.[11] The aircraft is to fly at Mach 1.5 and have a range of 5300 miles.

Detailed mission analysis for this aircraft has determined that one count of drag ($\Delta C_D = 0.0001$) is worth 310 lb of empty weight. This means that to optimize the range of the configuration we can minimize the objective function

$$I = \alpha C_D + \beta W \tag{2}$$

where C_D is the drag coefficient, W is the structural weight in pounds, and $\alpha/\beta = 3.1 \times 10^6$.

We parameterize the design using an arbitrary number of shape design variables that modify the outer-mold line (OML) of the aircraft and structural design variables that dictate the thicknesses of the structural elements. In this work the topology of the structure remains unchanged, that is, the number of spars and ribs and their planform-view location is fixed. However, the depth and thickness of the structural members are still allowed to change with variations of the OML.

Among the constraints to be imposed, the most obvious one is that during cruise the lift must equal the weight of the aircraft. In our optimization problem we constrain the C_L by periodically adjusting the angle of attack within the aerostructural solver.

We also must constrain the stresses so that the yield stress of the material is not exceeded at a number of load conditions. There are typically thousands of finite elements describing the structure of the aircraft, and it can become computationally very costly to treat these constraints separately. The reason for this high cost is that although there are efficient ways of computing sensitivities of a few functions with respect to many design variables and for computing sensitivities of many functions with respect to a few design variables, there is no known efficient method for computing sensitivities of many functions with respect to many design variables.

For this reason we lump the individual element stresses using Kreisselmeier–Steinhauser (KS) functions. In the limit all element stress constraints can be lumped into a single KS function, thus minimizing the cost of a large-scale aerostructural design cycle. Suppose that we have the following constraint for each structural finite element:

$$g_m = 1 - \sigma_m/\sigma_y \geq 0 \tag{3}$$

where σ_m is the von Mises stress in element m and σ_y is the yield stress of the material. The corresponding KS function is defined as

$$\text{KS} = -\frac{1}{\rho}\ln\left(\sum_m e^{-\rho g_m}\right) \tag{4}$$

This function represents a lower bound envelope of all of the constraint inequalities, where ρ is a positive parameter that expresses how close this bound is to the actual minimum of the constraints. This constraint lumping method is conservative and might not achieve the same result as treating the constraints separately. However, the use of KS functions has been demonstrated, and it constitutes a viable alternative, being effective in optimization problems with thousands of constraints.[12]

Having defined our objective function, design variables, and constraints, we can now summarize the aircraft design optimization problem as follows:

Minimize:

$$I = \alpha C_D + \beta W, \qquad \boldsymbol{x} \in \mathbb{R}^n$$

Subject to:

$$C_L = C_{L_T}, \qquad \text{KS} \geq 0, \qquad \boldsymbol{x} \geq \boldsymbol{x}_{\min}$$

The stress constraints in the form of KS functions must be enforced by the optimizer for aerodynamic loads corresponding to a number of flight and dynamic load conditions. Finally, a minimum gauge is specified for each structural element thickness.

Analytic Sensitivity Analysis

Our main objective is to calculate the sensitivity of a multidisciplinary function with respect to a number of design variables. The function of interest can be either the objective function or any of the constraints specified in the optimization problem. In general, such functions depend not only on the design variables, but also on the

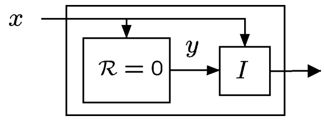

Fig. 3 Schematic representation of the governing equations ($\mathcal{R} = 0$), design variables x, state variables y, and objective function I, for an arbitrary system.

physical state of the multidisciplinary problem. Thus we can write the function as

$$I = I(\boldsymbol{x}, \boldsymbol{y}) \tag{5}$$

where $\boldsymbol{x}$ represents the vector of design variables and $\boldsymbol{y}$ is the state variable vector.

For a given set of design variables $\boldsymbol{x}$, the solution of the governing equations of the multidisciplinary system yields a state $\boldsymbol{y}$, thus establishing the dependence of the state of the system on the design variables. We denote these governing equations by

$$\boldsymbol{\mathcal{R}}[\boldsymbol{x}, \boldsymbol{y}(\boldsymbol{x})] = 0 \tag{6}$$

The first instance of $\boldsymbol{x}$ in the preceding equation indicates the fact that the residual of the governing equations might depend explicitly on $\boldsymbol{x}$. In the case of a structural solver, for example, changing the size of an element has a direct effect on the stiffness matrix. By solving the governing equations, we determine the state $\boldsymbol{y}$, which depends implicitly on the design variables through the solution of the system.

Because the number of equations must equal the number of state variables, $\boldsymbol{\mathcal{R}}$ and $\boldsymbol{y}$ have the same size. For a structural solver, for example, the size of $\boldsymbol{y}$ is equal to the number of unconstrained degrees of freedom, whereas for a computational-fluid-dynamics (CFD) solver this is the number of mesh points multiplied by the number of state variables at each point. For a coupled system $\boldsymbol{\mathcal{R}}$ represents all of the governing equations of the different disciplines, including their coupling.

A graphical representation of the system of governing equations is shown in Fig. 3, with the design variables $\boldsymbol{x}$ as the inputs and I as the output. The two arrows leading to I illustrate the fact that the objective function typically depends on the state variables and can also be an explicit function of the design variables.

When solving the optimization problem using a gradient-based optimizer, we require the total variation of the objective function with respect to the design variables, $\mathrm{d}I/\mathrm{d}\boldsymbol{x}$. As a first step towards obtaining this total variation, we use the chain rule to write the total variation of I as

$$\delta I = \frac{\partial I}{\partial \boldsymbol{x}}\delta \boldsymbol{x} + \frac{\partial I}{\partial \boldsymbol{y}}\delta \boldsymbol{y} \tag{7}$$

If we were to use this equation directly, the vector $\delta\boldsymbol{y}$ would have to be calculated by solving the governing equations for each component of $\delta\boldsymbol{x}$. If there are many design variables and the solution of the governing equations is costly (as is the case for large coupled iterative analyses), using Eq. (7) directly can be impractical.

We now observe that the variations $\delta\boldsymbol{x}$ and $\delta\boldsymbol{y}$ in the total variation of the objective function (7) are not independent of each other because the perturbed system must always satisfy the governing equations (6). A relationship between these two sets of variations can be obtained by realizing that the variation of the residuals (6) must be zero, that is,

$$\delta\boldsymbol{\mathcal{R}} = \frac{\partial \boldsymbol{\mathcal{R}}}{\partial \boldsymbol{x}}\delta \boldsymbol{x} + \frac{\partial \boldsymbol{\mathcal{R}}}{\partial \boldsymbol{y}}\delta \boldsymbol{y} = 0 \tag{8}$$

Because this residual variation (8) is zero, we can add it to the objective function variation (7) without modifying the latter, that is,

$$\delta I = \frac{\partial I}{\partial \boldsymbol{x}}\delta \boldsymbol{x} + \frac{\partial I}{\partial \boldsymbol{y}}\delta \boldsymbol{y} + \boldsymbol{\Psi}^T\left(\frac{\partial \boldsymbol{\mathcal{R}}}{\partial \boldsymbol{x}}\delta \boldsymbol{x} + \frac{\partial \boldsymbol{\mathcal{R}}}{\partial \boldsymbol{y}}\delta \boldsymbol{y}\right) \tag{9}$$

where $\boldsymbol{\Psi}$ is a vector of arbitrary scalars that we call the adjoint vector. This approach is identical to the one used in nonlinear constrained optimization, where equality constraints are added to the objective function, and the arbitrary scalars are known as Lagrange multipliers. The problem then becomes an unconstrained optimization problem, which is more easily solved.

We can now group the terms in Eq. (9) that contribute to the same variation and write

$$\delta I = \left(\frac{\partial I}{\partial \boldsymbol{x}} + \boldsymbol{\Psi}^T\frac{\partial \boldsymbol{\mathcal{R}}}{\partial \boldsymbol{x}}\right)\delta \boldsymbol{x} + \left(\frac{\partial I}{\partial \boldsymbol{y}} + \boldsymbol{\Psi}^T\frac{\partial \boldsymbol{\mathcal{R}}}{\partial \boldsymbol{y}}\right)\delta \boldsymbol{y} \tag{10}$$

If we set the term multiplying $\delta\boldsymbol{y}$ to zero, we are left with the total variation of I as a function of the design variables and the adjoint variables, removing the dependence of the total variation on the state variables. Because the adjoint variables are arbitrary, we can accomplish this by solving the adjoint equations

$$\frac{\partial \boldsymbol{\mathcal{R}}}{\partial \boldsymbol{y}}\boldsymbol{\Psi} = -\frac{\partial I}{\partial \boldsymbol{y}} \tag{11}$$

These equations depend only on the partial derivatives of both the objective function and the residuals of the governing equations with respect to the state variables. Because these partial derivatives do not depend on the design variables, the adjoint equations (11) only need to be solved once for each I and their solution is valid for all of the design variables.

When adjoint variables are found in this manner, we can use them to calculate the total sensitivity of I using the first term of Eq. (10), that is,

$$\frac{\mathrm{d}I}{\mathrm{d}\boldsymbol{x}} = \frac{\partial I}{\partial \boldsymbol{x}} + \boldsymbol{\Psi}^T\frac{\partial \boldsymbol{\mathcal{R}}}{\partial \boldsymbol{x}} \tag{12}$$

The cost involved in calculating sensitivities using the adjoint method is practically independent of the number of design variables. After having solved the governing equations, the adjoint equations (11) are solved only once for each I, and the vector products in the total derivative in Eq. (12) are relatively inexpensive.

It is important to realize the difference between the total and partial derivatives in this context. Partial derivatives can be evaluated without regard to the governing equations. This means that the state of the system is held constant when partial derivatives are evaluated, except, of course, when the denominator happens to be a state variable, in which case all but that particular state variable can kept constant. Total derivatives, on the other hand, take into account the solution of the governing equations that change the state $\boldsymbol{y}$. Therefore, when using finite differences, the cost of computing partial derivatives is usually a very small fraction of the cost involved in estimating total derivatives.

The partial derivative terms in the adjoint equations are therefore relatively inexpensive to calculate. The cost of solving the adjoint equations is similar to that involved in the solution of the governing equations.

The adjoint method has been widely used in several individual disciplines and examples of its application include structural sensitivity analysis[13] and aerodynamic shape optimization.[14–16]

Aerostructural Sensitivity Analysis

We now use the equations derived in the preceding section to write the adjoint sensitivity equations specific to the aerostructural system. In this case we have coupled aerodynamic and structural governing equations and two sets of state variables: the flow state vector and the vector of structural displacements. Figure 4 shows a diagram representing the coupling in this system. In the following expressions we split the vectors of residuals, states, and adjoints into two vectors corresponding to the aerodynamic and structural systems, that is,

$$\boldsymbol{\mathcal{R}} = \begin{bmatrix}\boldsymbol{\mathcal{A}}\\ \boldsymbol{\mathcal{S}}\end{bmatrix}, \qquad \boldsymbol{y} = \begin{bmatrix}\boldsymbol{w}\\ \boldsymbol{u}\end{bmatrix}, \qquad \boldsymbol{\Psi} = \begin{bmatrix}\psi\\ \phi\end{bmatrix} \tag{13}$$

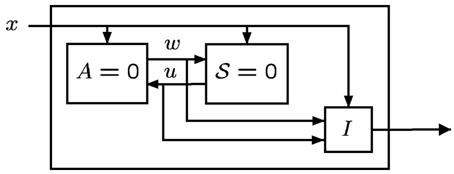

Fig. 4 Schematic representation of the aerostructural governing equations.

Using this notation, the adjoint equations (11) for an aerostructural system can be written as

$$\begin{bmatrix} \dfrac{\partial \boldsymbol{\mathcal{A}}}{\partial \boldsymbol{w}} & \dfrac{\partial \boldsymbol{\mathcal{A}}}{\partial \boldsymbol{u}} \\ \dfrac{\partial \boldsymbol{\mathcal{S}}}{\partial \boldsymbol{w}} & \dfrac{\partial \boldsymbol{\mathcal{S}}}{\partial \boldsymbol{u}} \end{bmatrix}^T \begin{bmatrix} \psi \\ \phi \end{bmatrix} = - \begin{bmatrix} \dfrac{\partial I}{\partial \boldsymbol{w}} \\ \dfrac{\partial I}{\partial \boldsymbol{u}} \end{bmatrix} \tag{14}$$

In addition to the diagonal terms of the matrix that appear when we solve the single-discipline adjoint equations, we also have off-diagonal terms that express the sensitivity of the governing equations of one discipline with respect to the state variables of the other. The residual sensitivity matrix in this equation is identical to that of the global sensitivity equations introduced by Sobieszczanski-Sobieski.[17] Considerable detail is hidden in the terms of this matrix, and, we describe each one of them for the sake of clarity.

1) The term $\partial \boldsymbol{\mathcal{A}}/\partial \boldsymbol{w}$ represents the variation of the CFD residuals caused by changes in the flow variables. When a flow variable at a given cell center is perturbed, the sum of the fluxes on that cell is altered. Only that cell and its neighbors are affected. Therefore, even though $\partial \boldsymbol{\mathcal{A}}/\partial \boldsymbol{w}$ is a large square matrix it is also extremely sparse, and its nonzero terms can be easily calculated. In our solvers this matrix is not stored explicitly.

2) The derivative $\partial \boldsymbol{\mathcal{A}}/\partial \boldsymbol{u}$ represents the effect of the structural surface displacements on the residuals of the CFD solution through the perturbation of the CFD mesh. When the wing deflects, the mesh must be warped, resulting in a change in the geometry of a subset of grid cells. Even though the flow variables are kept constant, the change in the geometry has an influence on the sum of the fluxes, whose variation is obtained by recalculating the residuals for the warped cells. If the residuals for all of the cells are recalculated, the cost of computing these partial derivatives is equal to the number of surface degrees of freedom of the structure times the cost of one aerodynamic residual computation. The total cost can be high when compared to the other partial derivatives; but given that the cost of one aerostructural solution is equivalent to about 1500 residual computations, the coupled-adjoint method is still worthwhile for problems where the number of surface degrees of freedom is not more than three-and-a-half orders of magnitude greater than the number of design variables.

3) The linear structural equations can be written as $\boldsymbol{\mathcal{S}} = \boldsymbol{K}\boldsymbol{u} - \boldsymbol{f} = 0$, where $\boldsymbol{K}$ is the stiffness matrix and $\boldsymbol{f}$ is the vector of applied forces. The only term that the flow variables affect directly is the applied force, and therefore the term $\partial \boldsymbol{\mathcal{S}}/\partial \boldsymbol{w}$ is equal to $-\partial \boldsymbol{f}/\partial \boldsymbol{w}$, which can be found by examining the procedure that integrates the pressures on the CFD surface mesh and transfers them to the structural nodes to obtain the applied forces.

4) Because the forces do not depend directly on the displacements and neither does $\boldsymbol{K}$ (for a linear model), the term $\partial \boldsymbol{\mathcal{S}}/\partial \boldsymbol{u}$ is simply the stiffness matrix $\boldsymbol{K}$.

The right-hand side terms in aerostructural adjoint equation (14) depend on the function of interest I. In our case we are interested in two different functions: the coefficient of drag C_D and the KS function. When $I = C_D$, we have the following:

1) The term $\partial C_D/\partial \boldsymbol{w}$ represents the direct sensitivity of the drag coefficient to the flow variables that can be obtained analytically by examining the numerical integration of the surface pressures that produce C_D.

2) The term $\partial C_D/\partial \boldsymbol{u}$ represents the change in the drag coefficient caused by the displacement of the wing while keeping the pressure distribution constant. The structural displacements affect the drag directly because they change the wing surface geometry over which the pressure distribution is integrated.

When $I = \text{KS}$, we have the following:

1) The term $\partial \text{KS}/\partial \boldsymbol{w}$ is zero because the stresses do not depend explicitly on the loads.

2) The stresses depend directly on the displacements because $\boldsymbol{\sigma} = S\boldsymbol{u}$. The term $\partial \text{KS}/\partial \boldsymbol{u}$ is therefore equal to $[\partial \text{KS}/\partial \boldsymbol{\sigma}]\boldsymbol{S}$.

Because the factorization of the full matrix in the coupled-adjoint equations (14) would be extremely costly, our approach uses an iterative solver, much like the one used for the aerostructural solution, where the adjoint vectors are lagged and the two different sets of equations are solved separately. For the calculation of the adjoint vector of one discipline, we use the adjoint vector of the other discipline from the preceding iteration, that is, we solve

$$\left[\frac{\partial \boldsymbol{\mathcal{A}}}{\partial \boldsymbol{w}}\right]^T \psi = -\frac{\partial I}{\partial \boldsymbol{w}} - \left[\frac{\partial \boldsymbol{\mathcal{S}}}{\partial \boldsymbol{w}}\right]^T \tilde{\phi} \tag{15}$$

$$\left[\frac{\partial \boldsymbol{\mathcal{S}}}{\partial \boldsymbol{u}}\right]^T \phi = -\frac{\partial I}{\partial \boldsymbol{u}} - \left[\frac{\partial \boldsymbol{\mathcal{A}}}{\partial \boldsymbol{u}}\right]^T \tilde{\psi} \tag{16}$$

where $\tilde{\psi}$ and $\tilde{\phi}$ are the lagged aerodynamic and structural adjoint vectors. The final result given by this system, is the same as that given by the original coupled-adjoint equations (14). We call this procedure the lagged-coupled adjoint method for computing sensitivities of coupled systems. Note that these equations look like the single discipline adjoint equations for the aerodynamic and the structural solvers, with the addition of forcing terms in the right-hand side that contain the off-diagonal terms of the residual sensitivity matrix. Note also that, even for more than two disciplines, this iterative solution procedure is nothing but the well-known block-Jacobi method.

As noted earlier, $\partial \boldsymbol{\mathcal{S}}/\partial \boldsymbol{u} = \boldsymbol{K}$ for a linear structural solver. Because the stiffness matrix is symmetric ($\boldsymbol{K}^T = \boldsymbol{K}$), the structural equations (16) are self-adjoint. Therefore, the structural solver can be used to solve for the structural adjoint vector ϕ by using the pseudoload vector given by the right-hand side of Eq. (16).

Once both adjoint vectors have converged, we can compute the final sensitivities of the objective function by using the following expression:

$$\frac{\mathrm{d}I}{\mathrm{d}\boldsymbol{x}} = \frac{\partial I}{\partial \boldsymbol{x}} + \psi^T \frac{\partial \boldsymbol{\mathcal{A}}}{\partial \boldsymbol{x}} + \phi^T \frac{\partial \boldsymbol{\mathcal{S}}}{\partial \boldsymbol{x}} \tag{17}$$

which is the coupled version of the total sensitivity equation (12). We now describe the last two partial derivatives in the preceding equation:

1) The term $\partial \boldsymbol{\mathcal{A}}/\partial \boldsymbol{x}$ represents the direct effect of aerodynamic shape perturbations on the CFD residuals, which is similar to that of the displacements on the same residuals ($\partial \boldsymbol{\mathcal{A}}/\partial \boldsymbol{u}$) that we mentioned earlier. The structural thicknesses of the structural finite elements do not affect the CFD residuals.

2) The design variables have a direct effect on both the stiffness matrix and the load. Although the partial derivative $\partial \boldsymbol{\mathcal{S}}/\partial \boldsymbol{x}$ is taken for a constant surface pressure field, a variation in the OML affects the translation of these pressures to structural loads. Hence, this partial derivative is equal to $[\partial \boldsymbol{K}/\partial \boldsymbol{x}]\boldsymbol{u} - \partial \boldsymbol{f}/\partial \boldsymbol{x}$.

For the $\partial I/\partial \boldsymbol{x}$ term we consider again two possibilities: $I = C_D$ and KS. For each of these cases, we have the following:

1) The term $\partial C_D/\partial \boldsymbol{x}$ is the change in the drag coefficient caused by wing-shape perturbations, while keeping the pressure distribution constant. This sensitivity is analogous to the partial derivative $\partial C_D/\partial \boldsymbol{u}$ that we just described and can be easily calculated by finite differencing the function that integrates the surface pressures to compute the drag coefficient. For structural variables that do not affect the OML, this term is zero.

2) The term $\partial \text{KS}/\partial \boldsymbol{x}$ represents the variation of the lumped stresses for fixed loads and displacements. When the OML is perturbed, the stresses in a given element can vary under these conditions if the shape is distorted.

As in the case of the partial derivatives in Eqs. (14), all of these terms can be computed without incurring a large computational cost because none of them involve the solution of the governing equations.

To solve the aircraft optimization problem we proposed, we also need sensitivities of the structural weight with respect to the design variables. Because the aerostructural coupling does not involve the weight, these sensitivities are easily computed.

Results

In this section we present the application of our sensitivity calculation method to the problem of aerostructural design of a supersonic, natural laminar-flow, business jet. Before presenting the results of our design experience, we describe the aerostructural analysis framework and a sensitivity validation study.

Aerostructural Analysis

The coupled-adjoint procedure is implemented in an aerostructural design framework previously developed by the authors.[7,10,18] The framework consists of an aerodynamic analysis and design module (which includes a geometry engine and a mesh perturbation algorithm), a linear finite element structural solver, an aerostructural coupling procedure, and various preprocessing tools that are used to set up aerostructural design problems. The multidisciplinary nature of this solver is illustrated in Fig. 5, where we can see the aircraft geometry, the flow solution and its associated mesh, and the primary structure inside the wing.

The aerodynamic analysis and design module, SYN107-MB,[15] is a multiblock parallel flow solver for both the Euler and the Reynolds-averaged Navier–Stokes equations that has been shown to be accurate and efficient for the computation of the flow around full aircraft configurations.[19] This package also includes an aerodynamic adjoint solver, which is able to perform aerodynamic shape optimization in the absence of aerostructural interaction.

The structural analysis package is FESMEH, a finite element solver developed by Holden.[20] The package is a linear finite element solver that incorporates two element types and computes the structural displacements and stresses of wing structures. Although this solver is not as general as some commercially available packages, it is still representative of the challenges involved in using large models with tens of thousands of degrees of freedom. High-fidelity coupling between the aerodynamic and the structural analysis programs is achieved using a linearly consistent and conservative scheme.[10,21]

The structural model of the wing is shown in Fig. 5 and is constructed using a wing box with six spars evenly distributed from 15 to 80% of the chord. Ribs are distributed along the span at every tenth of the semispan. A total of 640 finite elements were used in the construction of this model. Appropriate thicknesses of the spar caps, shear webs, and skins were chosen based on the expected loads for this design.

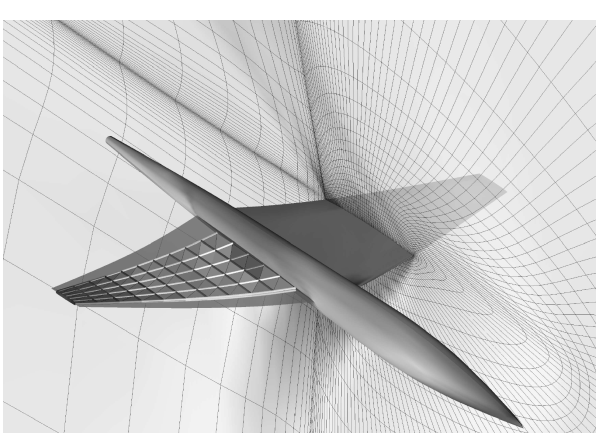

Fig. 5 Aerostructural model and solution of the supersonic business-jet configuration, showing a slice of the grid and the internal structure of the wing.

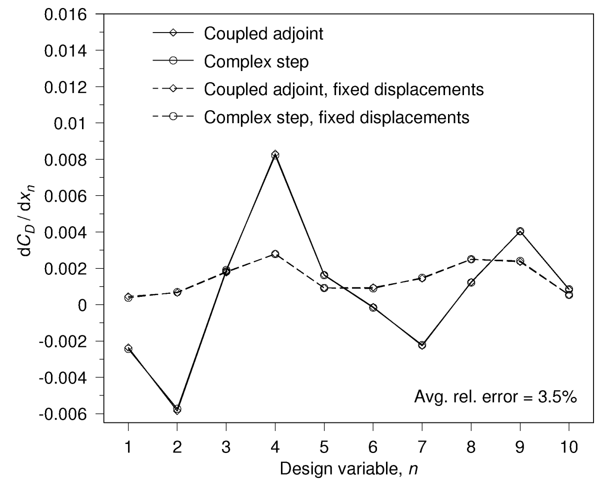

Fig. 6 Sensitivities of the drag coefficient with respect to shape perturbations.

Aerostructural Sensitivity Validation

To gain confidence in the effectiveness of the aerostructural coupled-adjoint sensitivities for use in design optimization, we must ensure that the values of the gradients are accurate. For validation purposes we use four sets of sensitivities. Results from the adjoint method are compared to the exact discrete value of these sensitivities using the complex-step derivative approximation.[22]

In this sensitivity study two different functions are considered: the aircraft drag coefficient C_D and the KS function (4). The sensitivities of these two quantities with respect to both OML shape design variables and structural design variables are computed and discussed.

C_D with Respect to OML Variables

The values of the aerostructural sensitivities of the drag coefficient with respect to shape perturbations are shown in Fig. 6. The 10 shape perturbations were chosen to be Hicks–Henne bumps distributed chordwise on the upper surface of two adjacent airfoils around the quarter span. The plot shows very good agreement between the coupled-adjoint and the complex-step results, with an average relative error between the two of only 3.5%. All of these sensitivities are total sensitivities in the sense that they account for the coupling between aerodynamics and structures.

To verify the need for taking the coupling into account, the same set of sensitivities was calculated for fixed structural displacements, where the displacement field is frozen after the aerostructural solution. This is similar to assuming that the wing, after the initial aeroelastic deformation, is held rigid as far as the computation of sensitivities is concerned. The calculation of the sensitivities only takes into account variations related to the aerodynamics. Figure 6 shows that the single-system sensitivities exhibit significantly lower magnitudes and even opposite signs for many of the design variables, when compared with the coupled sensitivities. The use of single-discipline sensitivities would clearly lead to erroneous design decisions.

C_D with Respect to Thickness Variables

Figure 7 also shows the sensitivity of the drag coefficient, this time with respect to the thicknesses of five skin groups and five spar groups distributed along the span. The agreement in this case is even better; the average relative error is only 1.6%. Even though these are sensitivities with respect to internal structural variables that do not modify the jig OML, the nonzero values in Fig. 7 demonstrate that coupled sensitivity analysis is needed.

KS with Respect to OML and Thickness Variables

The sensitivities of the KS function with respect to the two sets of design variables just described are shown in Figs. 8 and 9. The results show that the coupled-adjoint sensitivities are extremely accurate, with average relative errors of 2.9 and 1.6%. In Fig. 9 we

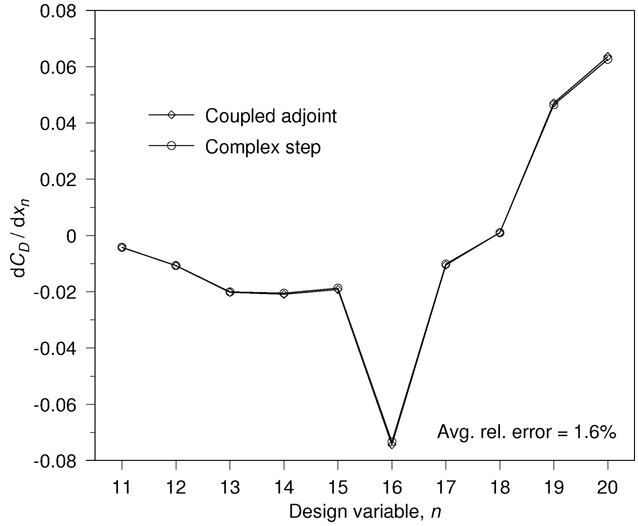

Fig. 7 Sensitivities of the drag coefficient with respect to structural thicknesses.

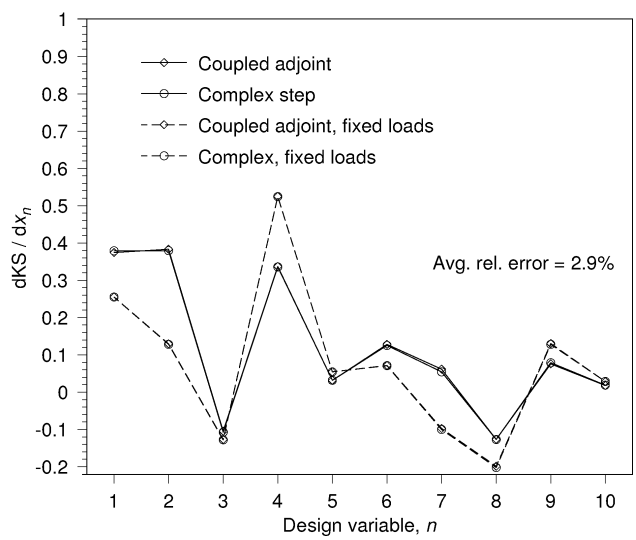

Fig. 8 Sensitivities of the KS function with respect to shape perturbations.

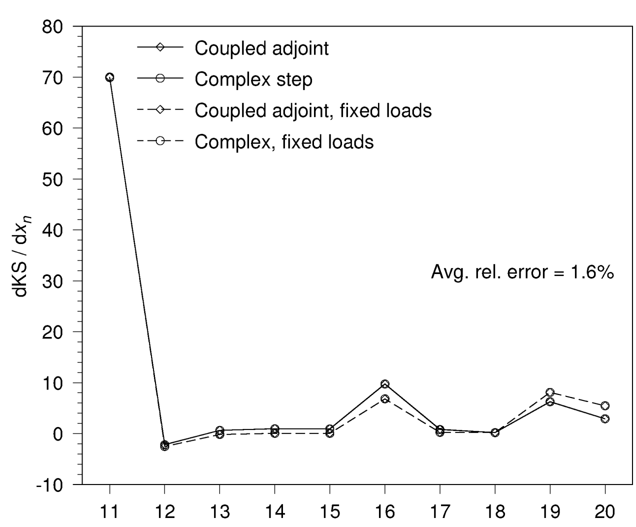

Fig. 9 Sensitivities of the KS function with respect to structural thicknesses.

observe that the sensitivity of the KS function with respect to the first structural thickness is much higher than the remaining sensitivities. This markedly different magnitude is because this particular structural design variable corresponds to the thickness of the top and bottom skins of the wing bay closest to the root, where the stress is the highest.

The sensitivities of the KS function for fixed loads are also shown in Figs. 8 and 9. Using the complex-step method, these sensitivities were calculated by calling only the structural solver after the initial aerostructural solution. The approach is equivalent to using just Eqs. (16) and (17) without the partial derivatives of $\boldsymbol{\mathcal{A}}$. The difference in these sensitivities when compared to the coupled ones is not as dramatic as in the fixed displacements case shown in Fig. 6, but it is still significant.

Aerostructural Design

The objective in this optimization is to solve the design problem that we described earlier, that is,

Minimize:

$$I = \alpha C_D + \beta W, \qquad \boldsymbol{x} \in \mathbb{R}^n$$

Subject to:

$$C_L = C_{L_T}, \qquad \mathrm{KS} \geq 0, \qquad \boldsymbol{x} \geq \boldsymbol{x}_{\min}$$

In our example the value of C_D corresponds to that of the cruise condition, which has a target lift coefficient of 0.1. The structural stresses, in the form of the KS function, correspond to a single maneuver condition, for which $C_{L_T} = 0.2$.

All optimization work is carried out using the nonlinear constrained optimizer NPSOL.[23] Euler calculations are performed on a wing-body 36-block mesh that is constructed from the decomposition of a $193 \times 33 \times 49$ C-H mesh. During the process of optimization, all flow evaluations are converged to 5.3 orders of magnitude of the average density residual, and the C_L constraint is satisfied within 10^{-6}.

To parameterize the shape of the aircraft, we have chosen sets of design variables that apply to both the wing and the fuselage. The wing shape is modified by the design optimization procedure at six defining stations uniformly distributed from the side of body to the tip of the wing. The shape modifications of these defining stations are linearly lofted to a zero value at the previous and next defining stations. On each defining station the twist, the leading- and trailing-edge camber distributions, and five Hicks–Henne bump functions on both the upper and lower surfaces are allowed to vary. The leading- and trailing-edge camber modifications are not applied at the first defining station. This yields a total of 76 OML design variables on the wing. Planform modifications, which are permitted by our software, were not used in the present calculations. Planform optimization is only meaningful if additional disciplines and constraints are taken into account.

The shape of the fuselage is parameterized in such a way that its camber is allowed to vary while the total volume remains constant. This is accomplished with nine bump functions evenly distributed in the streamwise direction starting at the 10% fuselage station. Fuselage nose and trailing-edge camber functions are added to the fuselage camber distribution in a similar way to what was done with the wing sections.

The structural sizing is accomplished with 10 design variables, which correspond to the skin thicknesses of the top and bottom surfaces of the wing. Each group is formed by the plate elements located between two adjacent ribs. All structural design variables are constrained to exceed a specified minimum gauge value.

The complete configuration is therefore parameterized with a total of 97 design variables. As mentioned in an earlier section, the cost of aerostructural gradient information using our coupled-adjoint method is effectively independent of the number of design variables: in more realistic full configuration test cases that we are about to tackle, 500 or more design variables will be necessary to describe the shape variations of the configuration (including nacelles, diverters, and tail surfaces) and the sizing of the structure.

Table 1 Comparison between the integrated and sequential approaches to aerostructural optimization

Design procedure	C_D, counts	KS	$\sigma_{\max}/\sigma_y$	ZFW, lbs	Range, n miles
Baseline	73.95	1.15×10^{-1}	0.87	47,500	6,420
Integrated optimization	69.22	-2.68×10^{-4}	0.98	43,761	7,361
Sequential optimization	——	——	——	——	——
Aerodynamic optimization					
Baseline	74.04	——	——	——	——
Optimized	69.92	——	——	——	——
Structural optimization					
Baseline	——	1.02×10^{-1}	0.89	47,500	——
Optimized	——	1.45×10^{-8}	0.98	44,782	——
Aerostructural analysis	69.92	-9.01×10^{-3}	0.99	——	7,137

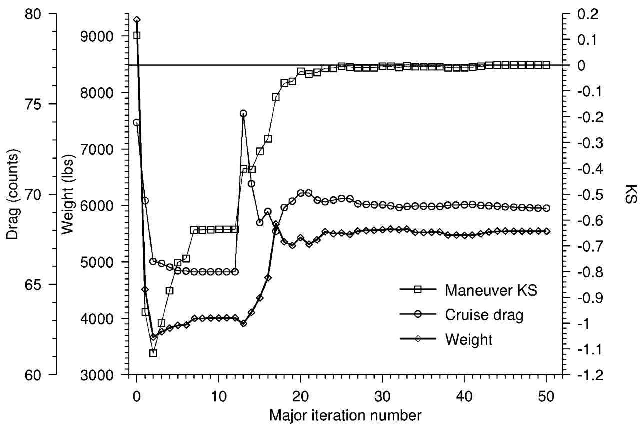

Fig. 10 Convergence history of the aerostructural optimization.

The initial application of our design methodology to the aerostructural design of a supersonic business jet is simply a proof-of-concept problem meant to validate the sensitivities obtained with our method. Current work is addressing the use of multiple realistic load conditions, dynamic loads, aeroelastic constraints, and the addition of diverters, nacelles, and empennage.

In the present design case we use $\alpha = 10^4$ and $\beta = 3.226 \times 10^{-3}$. Note that the scalars which multiply the structural weight W and the coefficient of drag C_D reflect the correct tradeoff between drag and weight that was already mentioned, that is, that one count of drag is worth 310 pounds of weight.

Figure 10 shows the evolution of this aerostructural design case for successive major design iterations. The figure shows the values of the coefficient of drag (in counts), the wing structural weight (in pounds), and the value of the KS function. Note that the structural constraints are satisfied when the KS function is positive. Because of the approximate nature of the KS function, all structural constraints can actually be satisfied for small but negative values of the KS function.

The baseline design is feasible, with a cruise drag coefficient of 74.04 counts and a structural weight of 9285 lbs. The KS function is slightly positive indicating that all stress constraints are satisfied at the maneuver condition. In the first two design iterations the optimizer takes large steps in the design space, resulting in a drastic reduction in both C_D and W. However, this also results in a highly infeasible design which exhibits maximum stresses that have a value of 2.1 times the yield stress of the material. After these initial large steps the optimizer manages to decrease the norm of the constraint violation. This is accomplished by increasing the structural skin thicknesses while decreasing the airfoil thicknesses, resulting in a weight increase and a further reduction in drag. Towards major iteration 10, there is no visible progress for several iterations while the design remains infeasible. In iteration 13 a large design step results in a sudden increase in feasibility accompanied by an equally sudden increase in C_D. The optimizer has established that the best way of obtaining a feasible design is to increase the wing thickness (with the consequent increases in C_D and weight) and the structural thicknesses. From that point on, the optimizer rapidly converges to the optimum. After 43 major iterations the KS constraint is reduced to $\mathcal{O}(10^{-4})$, and all stress constraints are satisfied. The aerostructurally optimized result has $C_D = 0.006922$ and a total wing structure weight of 5546 lbs.

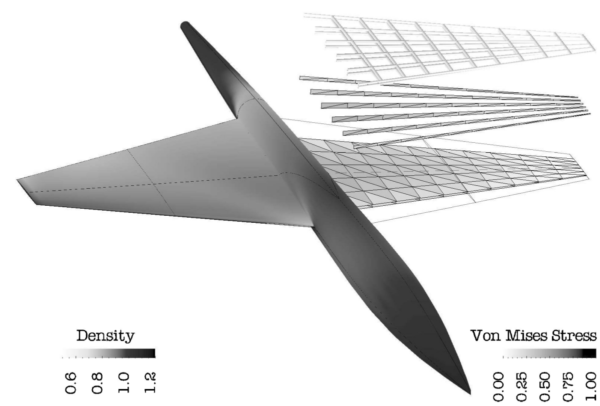

Fig. 11 Baseline configuration for the supersonic business jet showing surface densities at the cruise condition and structural stresses at the maneuver condition. The density is normalized by the freestream value, and the von Mises stresses are normalized by the material yield stress.

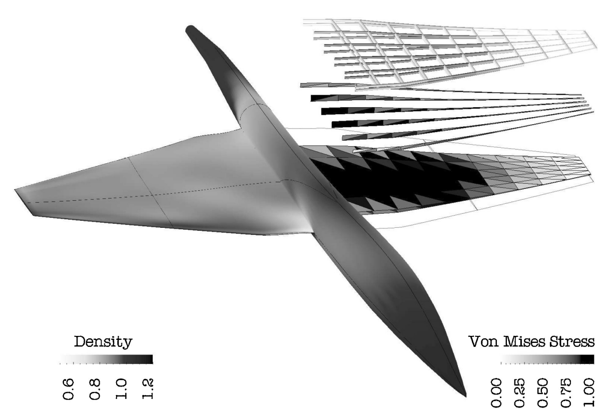

Fig. 12 Optimized configuration for the supersonic business jet.

Visualizations of the baseline and optimized configurations are shown in Figs. 11 and 12. Measures of performance and feasibility are presented in the first section of Table 1. The left halves of Figs. 11 and 12 show the surface density distributions with the corresponding structural deflections at the cruise condition for both the initial and optimized designs. The right halves show exploded views of the stress distributions on the structure (spar caps, spar shear webs, and skins, from top to bottom) at the $C_L = 0.2$ maneuver condition. From these figures one can appreciate that not only have the surface density distributions changed substantially at the cruise point, but so have the element stresses at the maneuver condition. In fact, as expected from a design case with a single load condition, the optimized structure exhibits stresses much closer to the yield stress, except in the outboard sections of the wing, where the minimum gauge constraints are active. About half of the improvement in the

C_D of the optimized configuration results from drastic changes in the fuselage shape: both front and aft camber have been added to distribute the lift more evenly in the streamwise direction in order to reduce the total lift-dependent wave drag.

A total of 50 major design iterations including aerostructural analyses, coupled-adjoint solutions, gradient computations, and line searches were performed in approximately 20 hours of wall clock time using 18 processors of an SGI Origin 3000 system (R12000, 400 MHz processors). Because these are not the fastest processors currently available, we feel confident that much larger models can be optimized with overnight turnaround in the near future.

Comparison with Sequential Optimization

The usefulness of a coupled aerostructural optimization method can only be measured by comparing with the results obtained using current state-of-the-art practices. In the case of aerostructural design, the typical approach is to carry out aerodynamic shape optimization with artificial airfoil thickness constraints meant to represent the effect of the structure, followed by structural optimization with a fixed OML. It is well known that sequential optimization cannot be guaranteed to converge to the true optimum of a coupled system. To determine the difference between the optima achieved by fully coupled and sequential optimizations, we have also carried out one cycle of sequential optimization within our analysis and design framework.

To prevent the optimizer from thinning the wing to an unreasonable degree during the aerodynamic shape optimization, five thickness constraints are added to each of the six defining stations for a total of 30 linear constraints. These constraints are such that, at the points where they are applied, the wing box is not allowed to get any thinner than the original design.

After the process of aerodynamic shape optimization is completed, the initial C_D has decreased to 0.006992, as shown in the lower portion of Table 1. After fixing the OML, structural optimization is performed using the maneuver loads for the baseline configuration at $C_L = 0.2$. The structural optimization process reduces the weight of the wing structure to 6567 lbs.

We can now compare the results of the fully coupled optimization in the preceding section and the outcome of the process of sequential optimization. The differences are clear: the coupled aerostructural optimization was able to achieve a design with a range of 7361 n miles, which is 224 n miles higher than that obtained from the sequential optimization.

Finally, because sequential optimization neglects the aerostructural coupling in the computation of maneuver loads there is no guarantee that the resulting design is feasible. In fact, the aerostructural analysis shows that the value of the KS function is slightly negative.

Conclusions

A methodology for coupled sensitivity analysis of high-fidelity aerostructural systems was presented. The sensitivities computed by the lagged-coupled-adjoint method were compared to sensitivities given by the complex-step derivative approximation and shown to be extremely accurate, having an average relative error of 2%. Moreover, significant differences in the values and signs of the sensitivities were found when aerostructural values were compared to rigid ones. In realistic aerostructural design problems with hundreds of design variables, there is a considerable reduction in computational cost when using the coupled-adjoint method as opposed to either finite differences or the complex-step approaches. This improvement is because the cost associated with the adjoint method is practically independent of the number of design variables.

Sensitivities computed using the presented methodology were successfully used to optimize the design of a supersonic business jet that was parameterized with a large number of aerodynamic and structural variables. The outcome of this optimization was compared with the traditional method of sequential optimization and it was found to improve the structural weight by an additional 16%.

Acknowledgments

The first author acknowledges the support of the Fundação para a Ciência e a Tecnologia from the Portuguese government and the Stanford University Charles Lee Powell Fellowship. The second author has benefited greatly from the support of the U.S. Air Force Office of Scientific Research under Grant AF-F49620-01-1-0291 and the Raytheon Aircraft Preliminary Design Group. Finally we would like to thank the ASSET Research Corporation for providing the geometry and specifications for the natural laminar-flow supersonic business jet.

References

[1]Sobieszczanski-Sobieski, J., and Haftka, R. T., "Multidisciplinary Aerospace Design Optimization: Survey of Recent Developments," *Structural Optimization*, Vol. 14, No. 1, 1997, pp. 1–23.

[2]Alexandrov, N., and Hussaini, M. Y. (eds.), *Multidisciplinary Design Optimization: State-of-the-Art*, SIAM, Philadelphia, 1997.

[3]Wakayama, S. R., "Lifting Surface Design Using Multidisciplinary Optimization," Ph.D. Dissertation, Dept. of Aeronautics and Astronautics, Stanford Univ., Stanford, CA, Dec. 1994.

[4]Bhatia, K. G., and Wertheimer, J., "Aeroelastic Challenges for a High Speed Civil Transport," AIAA Paper 93-1478, Feb. 1993.

[5]Giunta, A. A., "A Novel Sensitivity Analysis Method for High Fidelity Multidisciplinary Optimization of Aerostructural Systems," AIAA Paper 2000-0683, Jan. 2000.

[6]Maute, K., Nikbay, M., and Farhat, C., "Coupled Analytical Sensitivity Analysis and Optimization of Three-Dimensional Nonlinear Aeroelastic Systems," *AIAA Journal*, Vol. 39, No. 11, 2001, pp. 2051–2061.

[7]Reuther, J., Alonso, J. J., Martins, J. R. R. A., and Smith, S. C., "A Coupled Aero-Structural Optimization Method for Complete Aircraft Configurations," AIAA Paper 99-0187, Jan. 1999.

[8]Martins, J. R. R. A., Alonso, J. J., and Reuther, J., "Aero-Structural Wing Design Optimization Using High-Fidelity Sensitivity Analysis," *Proceedings—CEAS Conference on Multidisciplinary Aircraft Design Optimization*, edited by H. Hönlinger, Vol. 1, Lilienthal-Oberth e. V., Bonn, 2001, pp. 211–226.

[9]Martins, J. R. R. A., Alonso, J. J., and Reuther, J. J., "High-Fidelity Aero-Structural Design Optimization of a Supersonic Business Jet," AIAA Paper 2002-1483, April 2002.

[10]Martins, J. R. R. A., "A Coupled-Adjoint Method for High-Fidelity Aero-Structural Optimization," Ph.D. Dissertation, Dept. of Aeronautics and Astronautics, Stanford Univ., Stanford, CA, Oct. 2002.

[11]Kroo, I., Tracy, R., Chase, J., and Sturdza, P., "Natural Laminar Flow for Quiet and Efficient Supersonic Aircraft," AIAA Paper 2002-0146, Jan. 2002.

[12]Akgün, M. A., Haftka, R. T., Wu, K. C., and Walsh, J. L., "Sensitivity of Lumped Constraints Using the Adjoint Method," AIAA Paper 99-1314, April 1999.

[13]Adelman, H. M., and Haftka, R. T., "Sensitivity Analysis of Discrete Structural Systems," *AIAA Journal*, Vol. 24, No. 5, 1986, pp. 823–832.

[14]Jameson, A., "Aerodynamic Design via Control Theory," *Journal of Scientific Computing*, Vol. 3, No. 3, 1989, pp. 233–260.

[15]Reuther, J., Alonso, J. J., Jameson, A., Rimlinger, M., and Saunders, D., "Constrained Multipoint Aerodynamic Shape Optimization Using an Adjoint Formulation and Parallel Computers: Part I," *Journal of Aircraft*, Vol. 36, No. 1, 1999, pp. 51–60.

[16]Reuther, J., Alonso, J. J., Jameson, A., Rimlinger, M., and Saunders, D., "Constrained Multipoint Aerodynamic Shape Optimization Using an Adjoint Formulation and Parallel Computers: Part II," *Journal of Aircraft*, Vol. 36, No. 1, 1999, pp. 61–74.

[17]Sobieszczanski-Sobieski, J., "Sensitivity of Complex, Internally Coupled Systems," *AIAA Journal*, Vol. 28, No. 1, 1990, pp. 153–160.

[18]Martins, J. R. R. A., Alonso, J. J., and Reuther, J. J., "Complete Configuration Aero-Structural Optimization Using a Coupled Sensitivity Analysis Method," AIAA Paper 2002-5402, Sept. 2002.

[19]Reuther, J., Alonso, J. J., Vassberg, J. C., Jameson, A., and Martinelli, L., "An Efficient Multiblock Method for Aerodynamic Analysis and Design on Distributed Memory Systems," AIAA Paper 97-1893, June 1997.

[20]Holden, M. E., "Aeroelastic Optimization Using the Collocation Method," Ph.D. Dissertation, Dept. of Aeronautics and Astronautics, Stanford Univ., Stanford, CA, May 1999.

[21]Brown, S. A., "Displacement Extrapolation for CFD + CSM Aeroelastic Analysis," AIAA Paper 97-1090, Jan. 1997.

[22]Martins, J. R. R. A., Kroo, I. M., and Alonso, J. J., "An Automated Method for Sensitivity Analysis Using Complex Variables," AIAA Paper 2000-0689, Jan. 2000.

[23]Gill, P. E., Murray, W., and Saunders, M. A., "User's Guide for NPSOL (Version 5.0). A FORTRAN Package Nonlinear Programming," Stanford Univ., Dept. of Operations Research, TR SOL94-1, Stanford, CA, Nov. 1994.